



# Paradigm Shift for Radical *S*-Adenosyl-L-methionine Reactions: The Organometallic Intermediate $\Omega$ Is Central to Catalysis

Amanda S. Byer,<sup>†,¶</sup> Hao Yang,<sup>‡,¶</sup> Elizabeth C. McDaniel,<sup>†</sup> Venkatesan Kathiresan,<sup>‡</sup> Stella Impano,<sup>†</sup> Adrien Pagnier,<sup>†</sup> Hope Watts,<sup>†</sup> Carly Denler,<sup>†</sup> Anna L. Vagstad,<sup>§</sup> Jörn Piel,<sup>§</sup> Kaitlin S. Duschene,<sup>†</sup> Eric M. Shepard,<sup>†</sup> Thomas P. Shields,<sup>||</sup> Lincoln G. Scott,<sup>||</sup> Edward A. Lilla,<sup>⊥</sup> Kenichi Yokoyama,<sup>⊥</sup> William E. Broderick,<sup>†</sup> Brian M. Hoffman,<sup>\*,‡,¶</sup> and Joan B. Broderick<sup>\*,†,¶</sup>

<sup>†</sup>Department of Chemistry & Biochemistry, Montana State University, Bozeman, Montana 59717, United States

<sup>‡</sup>Department of Chemistry, Northwestern University, Evanston, Illinois 60208, United States

<sup>§</sup>Institute of Microbiology, Eidgenössische Technische Hochschule Zürich, Vladimir-Prelog-Weg 4, Zürich 8093, Switzerland

<sup>||</sup>Cassia, LLC, 3030 Bunker Hill Street, Ste. 214, San Diego, California 92109, United States

<sup>⊥</sup>Department of Biochemistry, Duke University Medical Center, Durham, North Carolina 27710, United States

## S Supporting Information

**ABSTRACT:** Radical *S*-adenosyl-L-methionine (SAM) enzymes comprise a vast superfamily catalyzing diverse reactions essential to all life through homolytic SAM cleavage to liberate the highly reactive 5'-deoxyadenosyl radical (5'-dAdo·). Our recent observation of a catalytically competent organometallic intermediate  $\Omega$  that forms during reaction of the radical SAM (RS) enzyme pyruvate formate-lyase activating-enzyme (PFL-AE) was therefore quite surprising, and led to the question of its broad relevance in the superfamily. We now show that  $\Omega$  in PFL-AE forms as an intermediate under a variety of mixing order conditions, suggesting it is central to catalysis in this enzyme. We further demonstrate that  $\Omega$  forms in a suite of RS enzymes chosen to span the totality of superfamily reaction types, implicating  $\Omega$  as essential in catalysis across the RS superfamily. Finally, EPR and electron nuclear double resonance spectroscopy establish that  $\Omega$  involves an Fe–C5' bond between 5'-dAdo· and the [4Fe–4S] cluster. An analogous organometallic bond is found in the well-known adenosylcobalamin (coenzyme B<sub>12</sub>) cofactor used to initiate radical reactions via a 5'-dAdo· intermediate. Liberation of a reactive 5'-dAdo· intermediate via homolytic metal–carbon bond cleavage thus appears to be similar for  $\Omega$  and coenzyme B<sub>12</sub>. However, coenzyme B<sub>12</sub> is involved in enzymes catalyzing only a small number (~12) of distinct reactions, whereas the RS superfamily has more than 100 000 distinct sequences and over 80 reaction types characterized to date. The appearance of  $\Omega$  across the RS superfamily therefore dramatically enlarges the sphere of bio-organometallic chemistry in Nature.

Radical *S*-adenosyl-L-methionine (SAM) enzymes comprise a vast superfamily, catalyzing diverse reactions essential to all life through homolytic SAM cleavage to liberate the highly reactive 5'-deoxyadenosyl radical (5'-dAdo·).<sup>1–3</sup> In the consensus mechanism for radical SAM (RS) enzymes,

electron-transfer to the sulfonium center of SAM from a reduced active-site [4Fe–4S] cluster causes reductive cleavage of the S–C(5') bond to directly liberate 5'-dAdo· for H atom abstraction from substrate (Figure S1).<sup>4–8</sup> However, this mechanism of radical initiation was put in question by the report of an organometallic reaction intermediate, denoted  $\Omega$ , in catalysis by the RS pyruvate formate-lyase activating enzyme (PFL-AE).<sup>9</sup> This intermediate, which has a carbon of 5'-dAdo· bonded to the unique Fe of the [4Fe–4S] cluster, formed subsequent to SAM cleavage, and 5'-dAdo· was only liberated through homolysis of the Fe–C bond of  $\Omega$ .<sup>9</sup> Here rapid freeze-quench (RFQ) EPR/ENDOR studies of a suite of enzymes, selected to collectively represent the broad range of RS superfamily reactions, implicate this organometallic intermediate as central to radical initiation across the RS superfamily. This leads us to propose a paradigm shift for radical initiation in these enzymes, that, with accompanying insights into the  $\Omega$  structure determination, mechanistically unifies the RS and adenosylcobalamin (coenzyme B<sub>12</sub>) enzymes: both involve homolysis of a metal–5'-deoxyadenosyl bond to liberate 5'-dAdo· for initiation of radical chemistry.

**1. Is  $\Omega$  the Result of Protein Conformational Rearrangements during Assembly of the PFL-AE/SAM/PFL Ternary Complex?** The observation of  $\Omega$  formation during rapid freeze-quench (RFQ) after mixing reduced PFL-AE with the two substrates, (PFL + SAM),<sup>9</sup> raised the possibility that  $\Omega$  was perhaps a means by which to store and control the nascent 5'-dAdo· during the complex conformational changes required for positioning of the target H atom as PFL-AE binds SAM and its 170 kDa substrate protein PFL.<sup>10–12</sup> To examine this possibility, we employed three different mixing conditions to RFQ trap intermediate states of the PFL-AE/SAM/PFL reaction (Figure 1). In all cases, reactions were RFQ trapped at 500 ms, as our previous work showed that  $\Omega$  formation was maximal at this time.<sup>9</sup> We repeated our original protocol,<sup>9</sup> rapid mixing of reduced PFL-

Received: April 16, 2018

Published: June 28, 2018

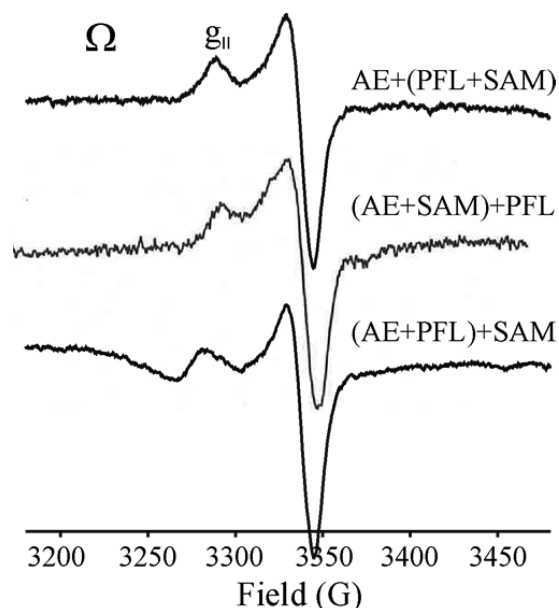


**Figure 1.** Top, premixed (PFL + SAM), RFQ with PFL-AE. Middle, (PFL-AE + SAM) RFQ with PFL. Bottom, (PFL-AE + PFL) + SAM; the slight increase in  $g_{||}$  suggests a slightly different conformation of  $\Omega$ . Feature to low field of  $\Omega$  signal in bottom spectrum due to  $\text{Cu}^{2+}$  contamination from Cu wheels used for freezing in RFQ apparatus. Conditions: Freeze-quenched, 500 ms; frequency, 9.374 GHz (top), 9.374 GHz (middle), 9.375 GHz (bottom); modulation, 10 G;  $T = 40$  K. Samples cryoannealed at 150 K to remove a small overlapping signal, see Figure S2.

AE with a solution that contained both the SAM and PFL substrates; in that case, both substrates must properly bind to PFL-AE prior to reaction. We then examined two other mixing conditions. In one, a solution of reduced (PFL-AE + SAM) was mixed with PFL; in this case, the SAM substrate is prebound but PFL has to bind after mixing. Finally, we prepared reduced (PFL-AE + PFL), thus preforming the PFL-AE/PFL complex with its attendant rearrangement of both proteins, and rapid-mixed with SAM. Figure 1 shows that in all three cases,  $\Omega$  is formed with its characteristic EPR axial signal, ( $g_{||} = 2.035$ ,  $g_{\perp} = 2.004$ ).<sup>9</sup> We conclude that in the PFL-AE catalyzed reaction, an extreme case of active-site and target protein rearrangement,<sup>11,12</sup>  $\Omega$  is a central intermediate that is formed regardless of the details/order of mixing.

**2. Is  $\Omega$  Mechanistically Formed throughout the RS Superfamily?** To test the intermediacy of  $\Omega$  broadly across the RS superfamily, we freeze-quench trapped intermediates in the reactions of PFL-AE and six additional canonical RS enzymes that perform diverse enzymatic functions representative of the entire superfamily (Figure 2).<sup>3</sup> First, these enzymes span the two major RS subclasses by including representatives that use SAM as a cosubstrate (PFL-AE, RNR-AE, HydG, PoyD and OspD) and those that use SAM as a cofactor (LAM and SPL).<sup>3</sup> Of the additional enzymes, two (RNR-AE<sup>13</sup> and SPL<sup>14</sup>) catalyze reactions on macromolecular substrates (anaerobic ribonucleotide reductase and DNA, respectively), two act on peptide substrates (PoyD and OspD),<sup>15</sup> two catalyze reactions of small molecule substrates (tyrosine for HydG<sup>16,17</sup> and lysine for LAM<sup>18</sup>), and finally one involves a second iron–sulfur cluster in catalysis (HydG).<sup>19</sup>

As described in Supporting Information, samples of all these diverse RS representatives were expressed in *Escherichia coli*,

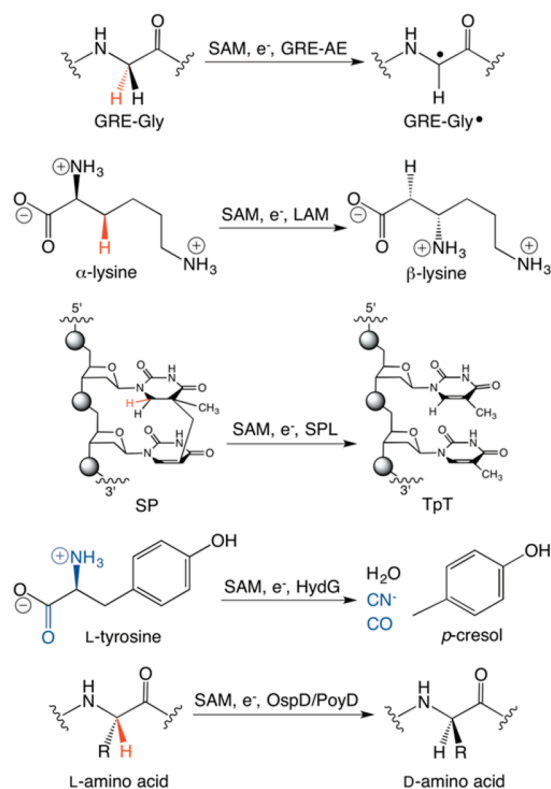


**Figure 2.** Reactions catalyzed by the radical SAM enzymes studied in this work. Glycyl radical enzyme activating enzyme (GRE-AE) refers to both PFL-AE and RNR-AE.

purified under anoxic conditions, subjected to Fe/S cluster reconstitution where necessary, photoreduced to generate the catalytically active  $[4\text{Fe}-4\text{S}]^{1+}$  cluster, rapid-mixed with a solution containing SAM and the appropriate substrate, and quenched 500 ms after mixing, followed by brief annealing at 150 K to remove a small contaminating signal (Figure S3). The resulting EPR spectra show that in every instance the reactant  $[4\text{Fe}-4\text{S}]^{1+}$  cluster signal has been completely replaced by the organometallic intermediate,  $\Omega$  (Figures 3, S3, S4). Moreover, we have initiated experiments to monitor how  $\Omega$  converts to product upon annealing, as previously shown for PFL-AE,<sup>9</sup> using representative enzymes from each of the two major RS subclasses, those using SAM as cosubstrate (RNR-AE, HydG) and as cofactor (LAM), and preliminary indications are that this occurs as anticipated (see Figure S5).

The  $\Omega$  spectra show slight variations from enzyme to enzyme in the shape of the  $g_{||}$  feature of this axial signal (Figure 3); these differences likely arise from small variations in the conformation of the intermediate, as seen in the  $\Omega$  signal for PFL-AE/PFL generated under different mixing conditions (Figure 1).

**3. Detailed Structure of  $\Omega$ .** With  $\Omega$  now identified as a ubiquitous RS intermediate, we carried out EPR and ENDOR measurements to refine the determination of its structure. Originally,  $\Omega$  was identified as involving the  $[4\text{Fe}-4\text{S}]$  cluster by its  $^{57}\text{Fe}$  ENDOR response.<sup>9</sup> The  $^{57}\text{Fe}$  line-broadening of the  $\Omega$  EPR signal (Figure S6), whose simulation requires inclusion of hyperfine interactions with multiple cluster  $^{57}\text{Fe}$  ions, further confirms that the spin of  $\Omega$  is carried by the  $[4\text{Fe}-4\text{S}]$  cluster. Incorporation of the dAdo fragment of SAM in  $\Omega$ <sup>9</sup> is confirmed here by observation of a loss of  $^1\text{H}$  ENDOR signals when  $\Omega$  is prepared with uniformly labeled  $[\text{D}_8\text{-ado}]\text{-SAM}$

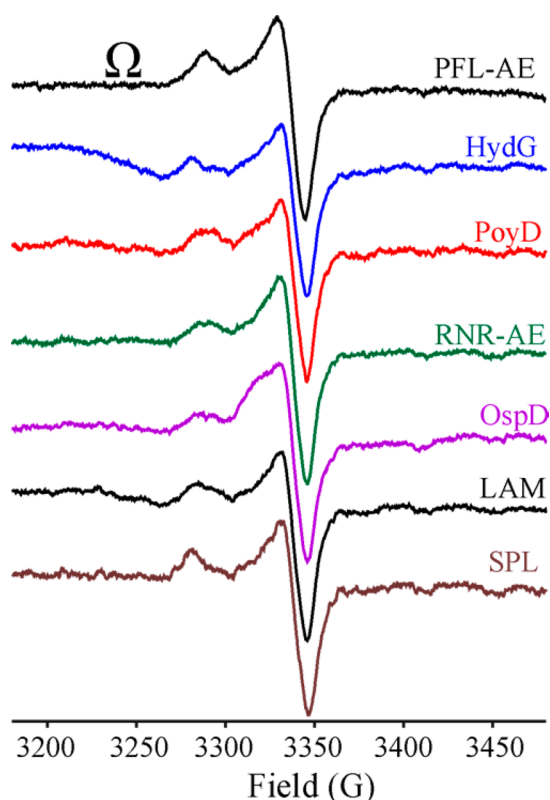


**Figure 3.** Normalized EPR spectra of  $\Omega$  formed in RS reactions freeze-quenched at 500 ms, taken after annealing 1 min at 150 K; spectra before annealing, Figure S3. RFQ-mixing condition: (substrate + SAM) + RS enzyme, freeze-quenched 500 ms after mixing. Conditions: frequency, 9.375 GHz; modulation amplitude, 10 G;  $T = 40$  K.

([adenosyl-2,8- $D_2$ -1',2',3',4',5',5''- $D_6$ ]-SAM) (Figure 4). The use of specifically labeled [5',5''- $D_2$ -ado]-SAM produces the

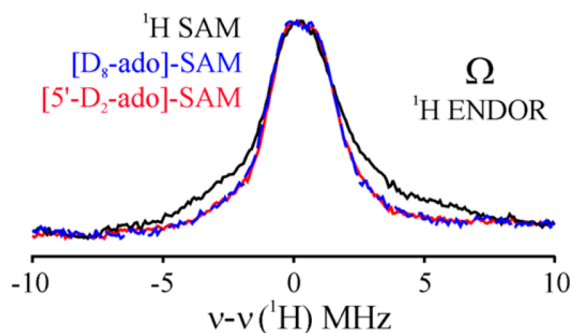


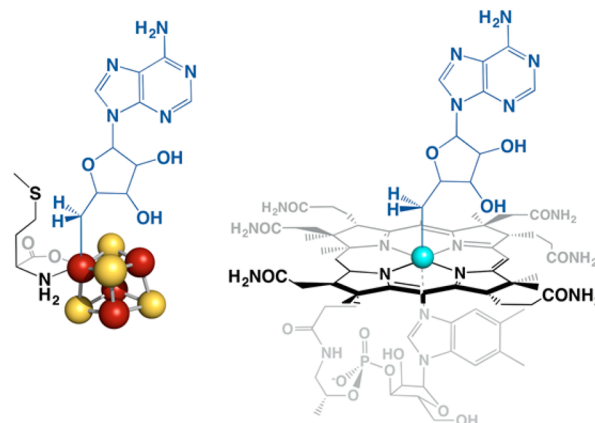
**Figure 4.** 35 GHz CW  $^1\text{H}$  ENDOR at  $g = 2.0134$  of  $\Omega$  for PFL-AE/PFL with (black)  $^1\text{H}$ -SAM; (blue-dashed) [D<sub>8</sub>-ado]-SAM ([adenosyl-2,8- $D_2$ -1',2',3',4',5',5''- $D_6$ ]-SAM); (red) [5',5''- $D_2$ -ado]-SAM ([adenosyl-5',5''- $D_2$ -SAM]). Mixing conditions: (PFL + SAM) + PFL-AE. ENDOR conditions: microwave frequency, 35.05 GHz; modulation amplitude, 0.5 G, +0.75 MHz/s;  $T = 2$  K.

same loss of  $^1\text{H}$  ENDOR signal as seen for  $\Omega$  made with uniformly [D<sub>8</sub>-ado]-SAM (Figure 4), unambiguously identifying the C5' carbon of 5'-dAdo $\cdot$  as forming the Fe–C bond in  $\Omega$ . Note that both the  $^1\text{H}$  coupling,  $A(^1\text{H}) \sim 7\text{--}8$  MHz, which also causes a distinct reduction in EPR line-width upon  $^2\text{H}$  replacement (Figure S7), and the previously observed  $^{13}\text{C}$  couplings from uniformly  $^{13}\text{C}$ -labeled SAM,  $a_{\text{iso}}(^{13}\text{C}) \sim 9$

MHz<sup>9</sup> are far too small to arise from an isolated 5'-dAdo $\cdot$ . Finally,  $^{14/15}\text{N}$ -Met-SAM give  $^{14/15}\text{N}$  ENDOR signals characteristic of direct coordination to the Fe,  $A(^{14}\text{N}) \approx 4$  MHz (Figure S8), confirming the retention of methionine coordination at the unique iron.

Together, these EPR/ENDOR observations leave no doubt that the  $\Omega$  EPR signal arises from an organometallic complex that contains a bond between a cluster Fe and the C5' carbon of 5'-dAdo $\cdot$ , with the methionine fragment of SAM anchored to the cluster via amino coordination, as shown in Chart 1

**Chart 1**



(left). The  $g$ -values of  $\Omega$  follow the pattern of a  $[4\text{Fe-4S}]^{3+}$  cluster,  $g_{\parallel} > g_{\perp} \gtrsim 2$ ,<sup>20</sup> which suggests a formal description of the intermediate as an  $[4\text{Fe-4S}]^{3+}$  cluster whose unique Fe is bound to the C5'-adenosyl carbanion (Chart 1). The resulting structure and reactivity of  $\Omega$  exhibit intriguing similarity to adenosylcobalamin (AdoCbl, coenzyme B<sub>12</sub>), which has a bond from the C5' carbon of a deoxyadenosyl moiety to the cobalt of cobalamin, Chart 1 (right), and undergoes homolytic Co–C bond cleavage to generate 5'-dAdo $\cdot$  to abstract an H from substrate.

#### 4. Mechanism: How does $\Omega$ Form, and Then Liberate 5'-dAdo $\cdot$ ?

Formation of  $\Omega$  might be indirect, (a) via reductive cleavage of SAM followed by combination of 5'-dAdo $\cdot$  with the unique Fe of the  $[4\text{Fe-4S}]^{2+}$  cluster (Figure 5, path 1); or it may occur in a single concerted step (Figure 5, path 2), via either (b) direct nucleophilic attack of the unique  $[4\text{Fe-4S}]^{1+}$  cluster Fe at the 5'-C of SAM; or (c) concerted reductive cleavage/ $\Omega$  formation initiated by interaction of the Fe with the SAM sulfur. The active site geometry of canonical RS enzymes places the S–C(S') bond of SAM *trans* to the Fe–S interaction (Figure 5).<sup>21</sup> This geometry is not conducive to nucleophilic attack of the unique Fe at the 5'-C of SAM to produce  $\Omega$ , thus disfavoring mechanism (b), but it would permit reductive cleavage routes (a) and (c) to form  $\Omega$  (Figure 5).<sup>22,23</sup> However, these two pathways themselves pose the perplexing question: why does 5'-dAdo $\cdot$  move toward the cluster and bind to the unique Fe to form  $\Omega$  upon cleavage of the S–C bond, rather than directly moving away and attacking the substrate? Given the active-site geometry, we suggest that  $\Omega$  formation is a direct mechanistic consequence of SAM activation for reductive cleavage by either routes (a) or (c): in both cases the SAM sulfur must migrate, in the transition state, toward the unique Fe of the  $[4\text{Fe-4S}]$  cluster, and when the S–C(S') bond breaks through reductive cleavage, the 5'-dAdo $\cdot$  fragment need only continue along this trajectory to interact

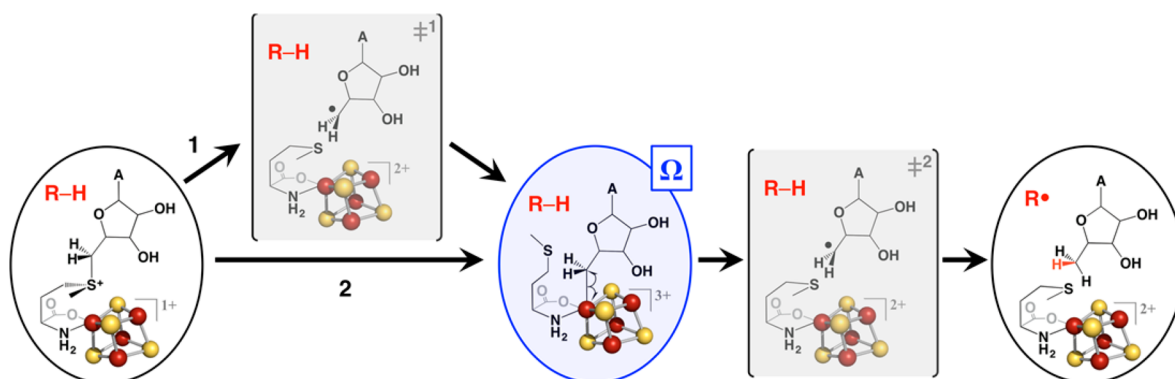


**Figure 5.** Pathways for liberating 5'-dAdo• for H atom abstraction through formation of catalytically competent  $\Omega$  upon SAM cleavage.  $\Omega$  may be formed via reductive SAM cleavage then recombination of the 5'-dAdo radical with the  $[4\text{Fe}-4\text{S}]^{2+}$  cluster (pathway 1), or directly (pathway 2) via concerted reductive cleavage/Fe-C bond formation or nucleophilic attack of the unique iron on the 5'-carbon. In addition, at present it cannot be excluded that a minority of the generated 5'-dAdo radical “escapes” to attack substrate directly, without  $\Omega$  formation.

with the unique iron and form  $\Omega$ . In a structural contrast, Lin and co-workers recently reported that in the noncanonical RS enzyme Dph2, the active-site architecture is set up for direct nucleophilic attack of the unique iron on the  $\text{C}\gamma(\text{met})$  to form a kinetically competent organometallic intermediate with an Fe-C( $\text{met}$ ) bond.<sup>24</sup> These considerations suggest why both Dph2 and canonical RS enzymes generate their key radical intermediates through prior formation of organometallic species,  $\Omega$  in the case of canonical RS enzymes.

How is the Fe-C( $\text{S}'$ ) bond of  $\Omega$  then activated to homolytically liberate 5'-dAdo• for reaction with substrate? This issue applies equally to the Co-C( $\text{S}'$ ) bond in the organometallic AdoCbl Co-C( $\text{S}'$ ) of  $\text{B}_{12}$ -radical enzymes, and this question in fact highlights not only the similarities but also the differences between AdoCbl and  $\Omega$ . The AdoCbl cofactor is a stable, isolable compound, and requires significant activation for Co-C( $\text{S}'$ ) bond homolysis.<sup>25,26</sup> In contrast,  $\Omega$  is a true reactive intermediate, and in PFL-AE,  $\Omega$  undergoes facile Fe-C bond cleavage even at low temperature ( $\sim 170$  K).<sup>9</sup>

The novel organometallic intermediate  $\Omega$ , whose structure is shown in Chart 1, forms in a suite of enzymes that represent the broad range of superfamily reactions, regardless of whether the enzymes consume SAM as cosubstrate or reuse SAM as cofactor, and independent of the size and complexity of the target substrate for H atom abstraction. This indicates that  $\Omega$  is a mechanistically central feature for radical initiation throughout the superfamily. In the long-held mechanism of radical initiation (Figure S1), reductive cleavage of SAM directly liberates 5'-dAdo•, which then abstracts a H atom from substrate.<sup>3</sup> Our results reveal a sharply different picture: liberation of the 5'-dAdo• for substrate H atom abstraction proceeds through the initial formation of  $\Omega$ , followed by homolytic cleavage of the Fe-C( $\text{S}'$ ) bond to liberate 5'-dAdo• for reaction (Figure 5). This is a paradigm shift for the mechanism of radical initiation by enzymes of the RS superfamily.

The identification of  $\Omega$  as integral to the mechanism of RS enzymes clearly unifies the RS and  $\text{B}_{12}$ -dependent radical-forming enzymes, despite the differences in reactivity of AdoCbl and  $\Omega$ : both utilize the cleavage of a metal-carbon bond (Chart 1) to liberate the reactive 5'-dAdo• for H atom abstraction from substrate. Our findings thus complete the integration of the two enzyme classes, as first contemplated by both Knappe<sup>27</sup> and Frey.<sup>28</sup> Beyond that, given the vast reach of

the RS superfamily across all domains of life,<sup>29</sup> these results dramatically enlarge the scope and importance of bioorganometallic chemistry in Nature.

## ■ ASSOCIATED CONTENT

### 📄 Supporting Information

The Supporting Information is available free of charge on the ACS Publications website at DOI: 10.1021/jacs.8b04061.

Supplemental methods and figures (PDF)

## ■ AUTHOR INFORMATION

### Corresponding Authors

\*[bmh@northwestern.edu](mailto:bmh@northwestern.edu)

\*[jbroderick@chemistry.montana.edu](mailto:jbroderick@chemistry.montana.edu)

### ORCID

Kenichi Yokoyama: 0000-0001-5625-469X

Brian M. Hoffman: 0000-0002-3100-0746

Joan B. Broderick: 0000-0001-7057-9124

### Author Contributions

¶These authors contributed equally to this work.

### Notes

The authors declare no competing financial interest.

## ■ ACKNOWLEDGMENTS

This work was funded by the NIH (GM 111097 to B.M.H.; GM 54608 to J.B.B.; GM 112838 to K.Y.), and by the U.S. Department of Energy (DE-SC0005404 to J.B.B. and E.M.S.).

## ■ REFERENCES

- (1) Sofia, H. J.; Chen, G.; Hetzler, B. G.; Reyes-Spindola, J. F.; Miller, N. E. *Nucleic Acids Res.* **2001**, *29*, 1097–1106.
- (2) Frey, P. A.; Hegeman, A. D.; Ruzicka, F. J. *Crit. Rev. Biochem. Mol. Biol.* **2008**, *43*, 63–88.
- (3) Broderick, J. B.; Duffus, B. R.; Duschene, K. S.; Shepard, E. M. *Chem. Rev.* **2014**, *114*, 4229–4317.
- (4) Frey, M.; Rothe, M.; Wagner, A. F. V.; Knappe, J. *J. Biol. Chem.* **1994**, *269*, 12432–12437.
- (5) Moss, M.; Frey, P. A. *J. Biol. Chem.* **1987**, *262*, 14859–14862.
- (6) Cheek, J.; Broderick, J. B. *J. Am. Chem. Soc.* **2002**, *124*, 2860–2861.
- (7) Magnusson, O. T.; Reed, G. H.; Frey, P. A. *J. Am. Chem. Soc.* **1999**, *121*, 9764–9765.
- (8) Horitani, M.; Byer, A. S.; Shisler, K. A.; Chandra, T.; Broderick, J. B.; Hoffman, B. M. *J. Am. Chem. Soc.* **2015**, *137*, 7111–7121.

(9) Horitani, M.; Shisler, K. A.; Broderick, W. E.; Hutcheson, R. U.; Duschene, K. S.; Marts, A. R.; Hoffman, B. M.; Broderick, J. B. *Science* **2016**, *352*, 822–825.

(10) Becker, A.; Fritz-Wolf, K.; Kabsch, W.; Knappe, J.; Schultz, S.; Wagner, A. F. V. *Nat. Struct. Biol.* **1999**, *6*, 969–975.

(11) Vey, J. L.; Yang, J.; Li, M.; Broderick, W. E.; Broderick, J. B.; Drennan, C. L. *Proc. Natl. Acad. Sci. U. S. A.* **2008**, *105*, 16137–16141.

(12) Peng, Y.; Veneziano, S. E.; Gillispie, G. D.; Broderick, J. B. *J. Biol. Chem.* **2010**, *285*, 27224–27231.

(13) Sun, X.; Eliasson, R.; Pontis, E.; Andersson, J.; Buist, G.; Sjöberg, B.-M.; Reichard, P. *J. Biol. Chem.* **1995**, *270*, 2443–2446.

(14) Rebeil, R.; Sun, Y.; Chooback, L.; Pedraza-Reyes, M.; Kinsland, C.; Begley, T. P.; Nicholson, W. L. *J. Bacteriol.* **1998**, *180*, 4879–4885.

(15) Morinaka, B. I.; Vagstad, A. L.; Helf, M. J.; Gugger, M.; Kegler, C.; Freeman, M. F.; Bode, H. B.; Piel, J. *Angew. Chem., Int. Ed.* **2014**, *53*, 8503–8507.

(16) Shepard, E. M.; Duffus, B. R.; McGlynn, S. E.; Challand, M. R.; Swanson, K. D.; Roach, P. L.; George, S. J.; Cramer, S. P.; Peters, J. W.; Broderick, J. B. *J. Am. Chem. Soc.* **2010**, *132*, 9247–9249.

(17) Driesener, R. C.; Challand, M. R.; McGlynn, S. E.; Shepard, E. M.; Boyd, E. S.; Broderick, J. B.; Peters, J. W.; Roach, P. L. *Angew. Chem., Int. Ed.* **2010**, *49*, 1687–90.

(18) Chirpich, T. P.; Zappia, V.; Costilow, R. N.; Barker, H. A. *J. Biol. Chem.* **1970**, *245*, 1778–1789.

(19) Driesener, R. C.; Duffus, B. R.; Shepard, E. M.; Bruzas, I. R.; Duschene, K. S.; Coleman, N. J.-R.; Marrison, A. P. G.; Salvadori, E.; Kay, C. W. M.; Peters, J. W.; Broderick, J. B.; Roach, P. L. *Biochemistry* **2013**, *52*, 8696–8707.

(20) Cutsail, G. E., III; Telsler, J.; Hoffman, B. M. *Biochim. Biophys. Acta, Mol. Cell Res.* **2015**, *1853*, 1370–1394.

(21) Vey, J. L.; Drennan, C. L. *Chem. Rev.* **2011**, *111*, 2487–2506.

(22) Kampmeier, J. A. *Biochemistry* **2010**, *49*, 10770–2.

(23) Nicolet, Y.; Amara, P.; Mouesca, J.-M.; Fontecilla-Camps, J. C. *Proc. Natl. Acad. Sci. U. S. A.* **2009**, *106*, 14867–14871.

(24) Dong, M.; Kathiresan, V.; Fenwick, M. K.; Torelli, A. T.; Zhang, Y.; Caranto, J.; Dzikovski, B.; Sharma, A.; Lancaster, K. M.; Freed, J. H.; Ealick, S. E.; Hoffman, B. M.; Lin, H. *Science* **2018**, *359*, 1247–1250.

(25) Banerjee, R. *Chem. Rev.* **2003**, *103*, 2083–94.

(26) Brown, K. L. *Chem. Rev.* **2005**, *105*, 2075–2149.

(27) Knappe, J.; Neugebauer, F. A.; Blaschkowski, H. P.; Gänzler, M. *Proc. Natl. Acad. Sci. U. S. A.* **1984**, *81*, 1332–1335.

(28) Frey, P. A. *FASEB J.* **1993**, *7*, 662–670.

(29) Akiva, E.; Brown, S.; Almonacid, D. E.; Barber, A. E.; Custer, A. F.; Hicks, M. A.; Huang, C. C.; Lauck, F.; Mashiyama, S. T.; Meng, E. C.; Mischel, D.; Morris, J. H.; Ojha, S.; Schnoes, A. M.; Stryke, D.; Yunes, J. M.; Ferrin, T. E.; Holliday, G. L.; Babbitt, P. C. *Nucleic Acids Res.* **2014**, *42*, D521–D530.